

# A novel CD34-derived hinge for rapid and efficient detection and enrichment of CAR T cells

Arthur Bister,<sup>1,2</sup> Tabea Ibach,<sup>1</sup> Corinna Haist,<sup>1,2</sup> Denise Smorra,<sup>2</sup> Katharina Roellecke,<sup>1</sup> Martin Wagenmann,<sup>1</sup> Kathrin Scheckenbach,<sup>1</sup> Norbert Gattermann,<sup>3</sup> Constanze Wiek,<sup>1,4</sup> and Helmut Hanenberg<sup>1,2,4</sup>

<sup>1</sup>Department of Otorhinolaryngology, Head & Neck Surgery, Heinrich Heine University, 40225 Düsseldorf, Germany; <sup>2</sup>Department of Pediatrics III, University Children's Hospital, University of Duisburg-Essen, Hufelandstrasse 55, 45147 Essen, Germany; <sup>3</sup>Department of Hematology, Heinrich Heine University, 40225 Düsseldorf, Germany

**Immunotherapy including chimeric antigen receptor (CAR) T cell therapy has revolutionized modern cancer therapy and has achieved remarkable remission and survival rates for several malignancies with historically dismal outcomes. The hinge of the CAR connects the antigen binding to the transmembrane domain and can be exploited to confer features to CAR T cells including additional stimulation, targeted elimination or detection and enrichment of the genetically modified cells. For establishing a novel hinge derived from human CD34, we systematically tested CD34 fragments of different lengths, all containing the binding site of the QBend-10 monoclonal antibody, in a FMC63-based CD19 CAR lentiviral construct. A final construct of 99 amino acids called C6 proved to be the best candidate for flow cytometry-based detection of CAR T cells and >95% enrichment of genetically modified T cells on MACS columns. The C6 hinge was functionally indistinguishable from the commonly used CD8 $\alpha$  hinge *in vitro* as well as in *in vivo* experiments in NSG mice. We also showed that the C6 hinge can be used for a variety of different CARs and mediates high killing efficacy without unspecific activation by target antigen-negative cells, thus making C6 ideally suited as a universal hinge for CARs for clinical applications.**

## INTRODUCTION

Chimeric antigen receptors (CARs) are part of a novel immunotherapeutic approach potentially suitable for a wide range of malignancies.<sup>1,2</sup> In CAR constructs, the single-chain variable fragment (scFv) of a monoclonal antibody (mAb) is linked with a hinge to a transmembrane region and at least one intracellular T cell activation motif, thereby combining antigen recognition and T cell activation in a single molecule.<sup>1,2</sup> Consequently, autologous T cells equipped with a CAR construct can detect and eliminate the target antigen-expressing tumor cells in a major histocompatibility complex-independent fashion.<sup>1,2</sup> In the last decade, major clinical breakthroughs have been achieved with CARs targeting CD19 and other antigens on B cell lineage-derived leukemia and lymphoma cells, which led to several CAR T cell therapies being approved in the United States and Europe for hematological malignancies.<sup>1-3</sup>

In CAR constructs, not only the scFv and the cytoplasmic signaling domains but also the hinge domain can greatly influence expres-

sion, stability and flexibility of the CAR and can enhance expansion as well as persistence of T cells.<sup>4-7</sup> Moreover, its length and flexibility are crucial for optimal recognition and binding to the antigen epitope by the scFv. Longer hinges are needed for recognizing target motifs, where the epitope is located proximal to the membrane of target cells or embedded within heavily glycosylated structures; shorter hinges are preferred when the epitope is located distal to the membrane and easily accessible.<sup>8-12</sup> Importantly, the hinge can also bind ligands itself. For example, constant heavy domains from human immunoglobulin G (IgG) have been used as hinges in CARs, but caused off-target toxicities due to binding to its natural receptors, Fc $\gamma$ RI, Fc $\gamma$ RII and Fc $\gamma$ RIII, on immune cells, which led to unspecific T cell activation, exhaustion and activation-induced cell death, ultimately resulting in insufficient disease control *in vivo* in animals.<sup>11,13</sup> Introducing mutations or truncations in the Fc $\gamma$ R binding domains can abrogate the off-target binding/activation and improved CAR function and efficacy.<sup>4,11,14</sup> Of note, the hinge in lisocabtagene maraleucel/JCAR017/Breyanzi, the US Food and Drug Administration (FDA)-approved CAR T cell therapy of Juno Therapeutics/Bristol Meyers Squibbs for CD19<sup>+</sup> B cell lymphomas, harbors a 12-amino acid (aa) IgG4 hinge without the CH<sub>2</sub>CH<sub>3</sub> sequence,<sup>11,15</sup> while the hinges in the other FDA-approved CAR T cell products are derived from CD28 (Yescarta, Tecartus) or from CD8 $\alpha$  (Kymriah).<sup>16</sup> The latter two antigens are both naturally expressed on T cells and thus can be considered safer for clinical use than the artificial expression of immunoglobulin protein sequences on T cells.

The hinge in CARs can facilitate elimination of the genetically modified T cells *in vivo* by including epitopes that can be specifically targeted, e.g., by administering mAbs such as rituximab<sup>17</sup> or by using CAR T cells that are redirected against the specific epitope in the hinge.<sup>18</sup> Other groups modified the hinge to include epitopes derived from CD34,<sup>17</sup> NGFR<sup>19</sup> or artificial sequences such as Strep-Taq II<sup>20</sup> to

Received 4 August 2021; accepted 8 November 2021;  
<https://doi.org/10.1016/j.omto.2021.11.003>.

<sup>4</sup>These authors contributed equally

**Correspondence:** Helmut Hanenberg, MD, Department of Pediatrics III, University Children's Hospital, University of Duisburg-Essen, Hufelandstrasse 55, 45122 Essen, Germany.

**E-mail:** [helmut.hanenberg@uk-essen.de](mailto:helmut.hanenberg@uk-essen.de)



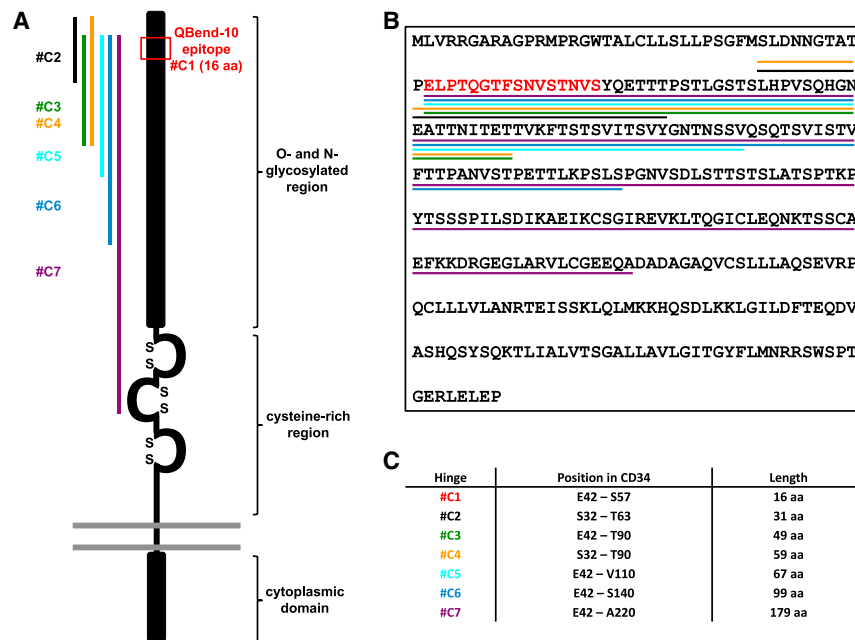


**Figure 1. Structure and amino acid sequence of human CD34**

(A) Human CD34 consists of a heavily O- and N-glycosylated region followed by a six-cysteine rich domain with three IgG-like domains and a cytoplasmic domain. The 16 aa QBend-10 epitope (#C1) is located close to the N terminus and the newly derived hinges #C2–#C7 are designed around this epitope. (B) Full amino acid sequence of human CD34. The critical 16 aa stretch is marked in red. Amino acid sequences of hinges #C2–#C7 are underlined in the corresponding color. (C) Overview of the length and position within the CD34 molecule of #C1–#C7.

## RESULTS

### Vector, CAR and hinge design

The CD34 MACS enrichment system from Miltenyi Biotec is based on the CD34 antibody clone QBend-10 recognizing a well-defined 16-aa sequence, ELPTQGTFSNVSTNVS,<sup>34</sup> which we named C1 and that is located in a heavily O- and N-glycosylated region of the protein (Figure 1A). We first designed six hinges of different lengths by adding amino acid stretches from the wild-type protein up- and/or downstream of the

QBend-10 recognition site in CD34, labeled as C2 (31 aa), C3 (49 aa), C4 (59 aa), C5 (67 aa), C6 (99 aa) and C7 (179 aa), shown in Figures 1B and 1C.

### Expression and enrichment of CD34-hinged CARs in Jurkat cells

The CD34 fragments C2–C7 were cloned as hinges into our previously published CD19 CAR lentiviral vector, which co-expresses the enhanced green fluorescent protein (EGFP) and a human codon usage-optimized FMC63-based second-generation CAR construct with the transmembrane and cytoplasmic region of human CD28 via a T2A site under the control of the MPSV promoter (Figure 2A).<sup>35</sup> To test whether cells expressing CD34-hinged CARs can be detected by antibody staining and can be enriched by CD34 microbeads, Jurkat cells were transduced with the six lentiviral CD19 CAR constructs harboring C2–C7 as hinges. Flow-cytometric analysis of the transduced Jurkat cells stained with the QBend-10 CD34-PE antibody revealed that EGFP expression for all six constructs strongly correlated with the CAR expression levels (Figure 2B). Next, batches of transduced Jurkat cells were incubated with CD34 microbeads and subjected to one round of enrichment on MACS columns. Prior to the enrichments, the transduction efficiencies for C2-, C3-, C4-, and C5-hinged CARs were very similar ( $61.6\% \pm 2.7\%$  to  $68.7\% \pm 2.7\%$ ), while C6-hinged CARs showed the lowest,  $50.7\% \pm 10.5\%$ , and C7-hinged constructs the highest transduction efficiency of  $78.4\% \pm 3.2\%$  (Figure 2C; preMACS). For all hinges, the enrichment with CD34 microbeads led to EGFP<sup>+</sup> populations well above 90%, with C4, C5 and C7 having the purest postMACS populations, 97.8%, 97.1%, and 98.8%, respectively (Figure 2C; postMACS). However, compared with the percentages of EGFP<sup>+</sup> cells prior to MACS

enable enrichment as well as flow-cytometric detection of CAR T cells. Flow cytometry, especially in research settings, is optimally suited for determining the immunological phenotypes of CAR-expressing cells and also for comparing the expression patterns of different CAR constructs on the transgenic immune effector cells.<sup>14,19</sup> In clinical settings, these analyses are often much more laborious and rely on qRT-PCR<sup>21,22</sup> droplet digital PCR,<sup>23</sup> RNA sequencing,<sup>24</sup> positron emission tomography,<sup>25</sup> antibodies against the scFv<sup>26,27</sup> linkers between heavy and light chain,<sup>28</sup> Fc-tagged antigens<sup>23,29</sup> or the expression of separate cell-surface marker genes co-expressed in the CAR lentiviral constructs, e.g., truncated epidermal growth factor receptor.<sup>15,30</sup>

When designing a new hinge for potential clinical purposes, we considered the human CD34 adhesion molecule to be ideally suited as candidate, as CD34 is of human origin and not expressed on mature immune effector cells, including human T and natural killer (NK) cells; also the natural ligands for CD34, CD62L, CD62E and CD62P, are well known.<sup>31</sup> GMP-grade immunomagnetic CD34 enrichment reagents (MACS; Miltenyi Biotec) are commercially available and have been used for more than 15 years to enrich CD34<sup>+</sup> hematopoietic stem cells from different source materials for human stem cell transplantation without the need to remove the microbeads from the infused products.<sup>32,33</sup> The aim of this work was to systematically establish a human CD34-derived hinge for CAR constructs, which facilitates to routinely enrich CAR T cells to high purities and which functions well in a variety of CAR constructs *in vitro* and *in vivo* comparably to a clinically used human CD8-derived hinge.

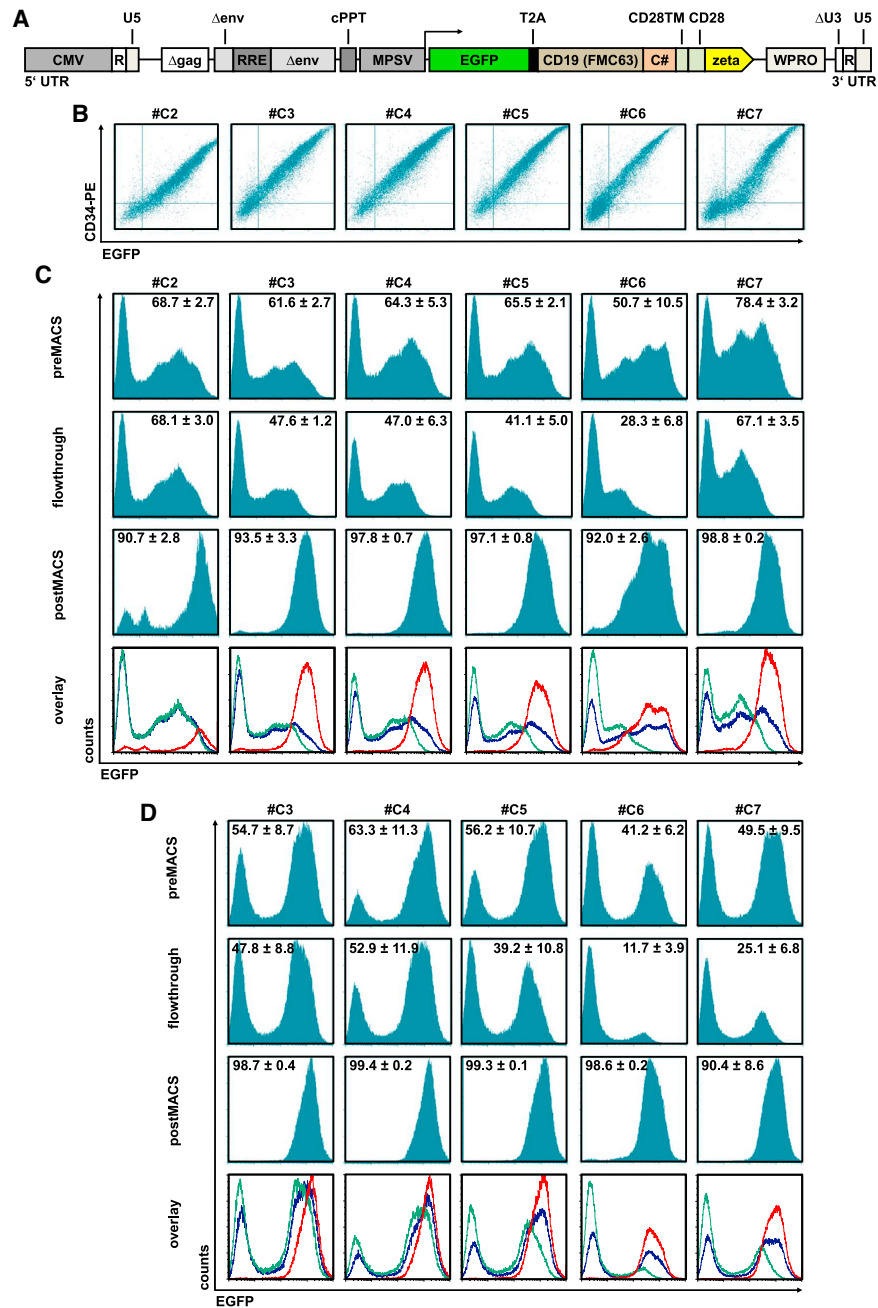


### Figure 2. CD34-hinged CAR expression and enrichment

Jurkat or primary human T cells were lentivirally transduced with VSVG-pseudotyped vectors encoding EGFP in *cis* with  $\Delta$ CD34-hinged CD19 CARs (vector depicted schematically in A). (B) Three days after transduction, Jurkat cells were flow-cytometrically analyzed for CAR (via CD34-PE) and EGFP expression.  $\Delta$ CD34-hinged CD19 CAR (C) Jurkat or (D) primary human T cells were enriched via magnetic cell sorting using CD34 microbeads, and the three fractions (preMACS, flowthrough, and postMACS) were analyzed for EGFP expression by flow cytometry. In the overlay, preMACS is depicted as a blue line, the flowthrough as a green line, and postMACS as a red line. Representative blots were used. Values indicate the percentages of CAR-positive cells and are shown as means  $\pm$  SEM from at least three experiments.

selection, the enrichments of C2–C5 hinged CARs were quite inefficient, as the majority of the CAR-expressing cells was lost in the flowthrough (Figure 2C; flowthrough). Here, the C6 hinge proved to be most efficient for selection purposes, as only 28.3% out of

50.7% (55.8%) mostly low EGFP-expressing CAR cells were present in the flowthrough of the columns and 92.0% transduced cells could be eluted from the columns. Due to the high inefficiency for selection on MACS columns, the C2-hinge construct was not further analyzed.

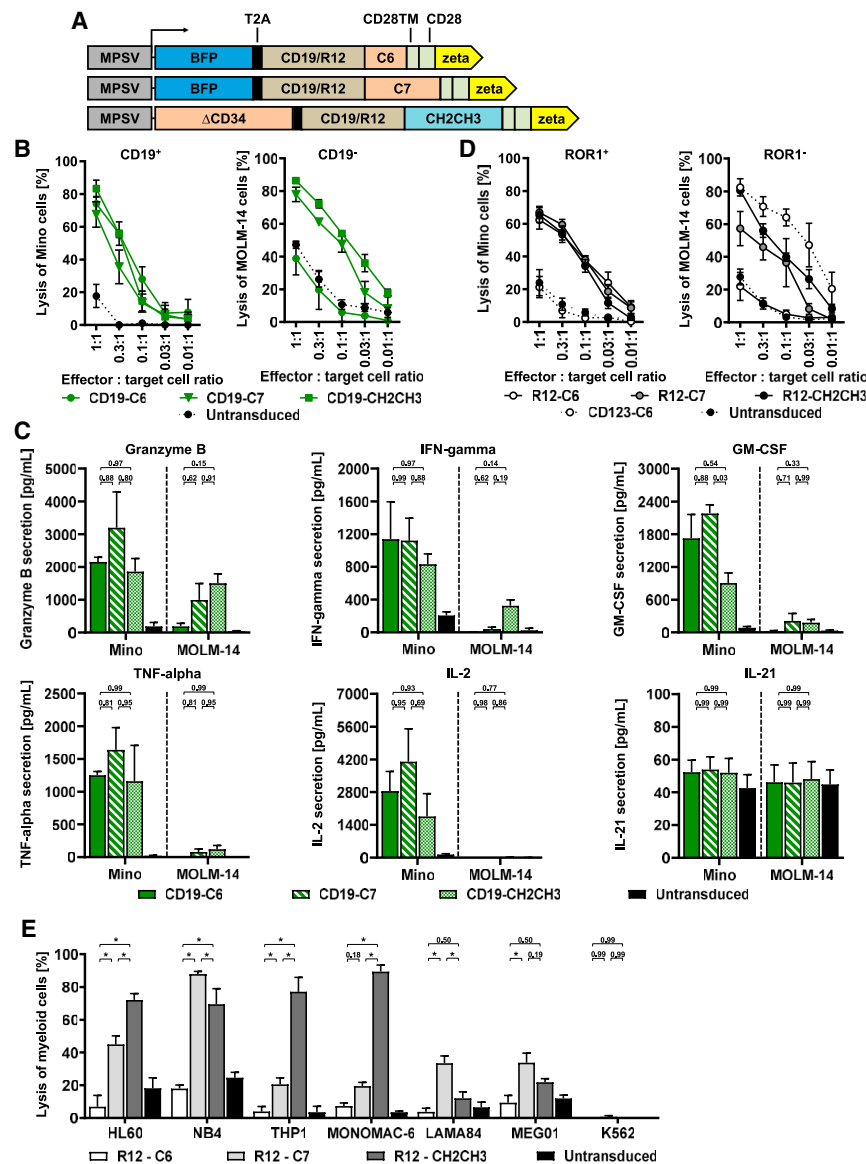


**Figure 3. Comparison of C6- and C7-hinged CD19 and R12 CARs with CH<sub>2</sub>CH<sub>3</sub>-hinged counterparts**

Primary human T cells were lentivirally transduced with VSVG-pseudotyped vectors encoding BFP in *cis* with C6- or C7-hinged or ΔCD34 in *cis* with CH<sub>2</sub>CH<sub>3</sub>-hinged CD19 or R12 CARs (vectors depicted schematically in A). Three days after transduction, the CAR T cells were enriched via MACS and subsequently co-cultured with (B and D) EGFP-expressing Mino or MOLM-14 cells at decreasing effector-to-target cell ratios or (E) with various myeloid cell lines at an effector-to-target cell ratio of 1:1. After 16 h, the target cell lysis was assessed by flow cytometry and (C) supernatants were harvested and analyzed for granzyme B, IFN-γ, GM-CSF, IL-2, TNF-α and IL-21 secretion via the cytotoxic T and NK cell MACSplex cytokine assay. P values were calculated by two-way ANOVA (B, D, and E) or one-way ANOVA (C) followed by Tukey's or Dunnett's multiple comparison testing, respectively; asterisks indicate p values of <0.05; the p values of the lysis curves are summarized in Table S1. Data are presented as means ± SEM of at least three biological replicates.

lost in the flowthrough of the columns (Figure 2D; flowthrough). The C6 hinge with 99 aa proved to be highly efficient to retain the majority of CAR T cells on the MACS column, as only 11.7% out of 41.2% (28.4%) of T cells with low expression of EGFP/CAR were detectable in the flowthrough (Figure 2D). With respect to the ability to retain the CAR T cells on the column, the C7 construct came in as the second best with slightly lower purity (90.4%).

**Killing efficacy and specificity of CD19 CARs with C6, C7, or CH<sub>2</sub>CH<sub>3</sub> hinges**

As the CH<sub>2</sub>CH<sub>3</sub> fragments of human IgG1 or IgG4 have been commonly used as hinges for CARs,<sup>11,14</sup> we next compared the cytotoxic efficacy and specificity of CD19 CAR T cells with the C6 or C7 hinges against a corresponding

CH<sub>2</sub>CH<sub>3</sub>-hinged CAR construct. To enable enrichment of the transduced T cells on MACS columns in this set of experiments, we transduced primary human T cells with vectors encoding blue fluorescent protein (BFP) in *cis* with C6- or C7-hinged or the previously described ΔCD34,<sup>35</sup> which is truncated after the transmembrane domain and thus lacks the signaling domains, in *cis* with CH<sub>2</sub>CH<sub>3</sub>-hinged CD19 CARs (Figure 3A). The CAR T cells were enriched via CD34 MACS to >90% and then co-cultured with the CD19<sup>+</sup> ROR1<sup>+</sup> mantle cell lymphoma (MCL) cell line Mino or the CD19<sup>-</sup> ROR1<sup>-</sup> acute myeloid leukemia (AML) cell line MOLM-14 (Figure S1) for 16 h with subsequent cytotoxicity and cytokine secretion measurements. We also included a CD123 CAR<sup>36</sup> with the C6 hinge in these experiments, which served as a negative control for Mino and a positive control for MOLM-14 cells.

**Expression and enrichment of CD34-hinged CARs in primary T cells**

Next, primary human T cells were transduced with the C3–C7-hinged CD19 CAR lentiviral constructs. Three days later, the T cells were harvested, stained with CD34 microbeads and subjected to enrichment for CAR-expressing cells on MACS columns. Flow-cytometric analysis of the T cell cultures prior to selection demonstrated that the transduction efficiencies ranged between 41.2% ± 6.2% for the C6 construct and 63.3% ± 11.3% for C4 (Figure 2D; preMACS). One run over the MACS columns was sufficient to enrich the CAR-positive T cells to high purities between 90.4% ± 8.6% for C7 and 99.4% ± 0.2% for C4 (Figure 2D; postMACS). Similar to the experiments with Jurkat, the use of the shorter hinges C3–C5 was associated with inefficient enrichment of transduced cells, as the majority of CAR T cells was

All three CD19 CAR constructs showed comparable cytotoxicity when expressed on T cells (Figure 3B) and also comparable secretion of granzyme B, interferon- $\gamma$  (IFN- $\gamma$ ), granulocyte macrophage colony-stimulating factor (GM-CSF), tumor necrosis factor  $\alpha$  (TNF- $\alpha$ ) and interleukin-2 (IL-2) against Mino cells (Figure 3C). Similarly, T cells expressing the C6-, C7- and CH<sub>2</sub>CH<sub>3</sub>-hinged ROR1 CARs based on the mAb clone R12<sup>37</sup> equally efficaciously eliminated Mino cells (Figure 3D). In contrast, when using a CAR construct based on the ROR1 mAb clone R11, which targets a membrane-proximal epitope,<sup>37</sup> only the long CH<sub>2</sub>CH<sub>3</sub> hinge mediated recognition and killing of Mino cells (Figure S2A).

The CD19<sup>-</sup> and ROR1<sup>-</sup> MOLM-14 cell line was nonspecifically lysed by C7- and CH<sub>2</sub>CH<sub>3</sub>-hinged CARs, including the R11-C7 CAR, but not by C6-hinged CD19 or ROR1 CARs (Figures 3B and 3D; Figure S2A). Importantly, the off-target toxicity of C7- and CH<sub>2</sub>CH<sub>3</sub>-hinged CARs was not restricted to MOLM-14 cells, but also occurred when the R12-C7 (but not R12-C6) CAR T cells were incubated with other ROR1<sup>-</sup> acute and chronic myeloid leukemia cell lines (Figure 3E). Consistent with the lysis data, CD19-C7 and CD19-CH<sub>2</sub>CH<sub>3</sub>, but not CD19-C6 CAR T cells secreted granzyme B and also low levels of IFN- $\gamma$ , GM-CSF, and TNF- $\alpha$  after co-culture with MOLM-14 cells (Figure 3C). While the CH<sub>2</sub>CH<sub>3</sub>-mediated lysis of MOLM-14 was presumably caused by the binding of the CH<sub>2</sub>CH<sub>3</sub> hinge to Fc receptors on MOLM-14,<sup>14</sup> the reason for C7-mediated CAR T cell activation was unknown. Nevertheless, we were able to exclude CD34 microbeads stuck to the C7 hinge as an inducer of the off-target toxicity, as the unspecific activation of C7-hinged CD19 CAR T cells also occurred when MOLM-14 cells were co-cultured with non-enriched CAR T cells (Figure S2B).

#### CD34 glycosylation plays no role for the activation of C7-hinged CARs by AML blasts

Post-translational modifications of the adhesion molecule CD34 and its main ligand on leukocytes, L-selectin, are essential for homing of leukocytes to several organ systems and occur by N-linked or O-linked glycosylation of CD34.<sup>38,39</sup> Importantly, for the adhesion mediated by L-selectin, CD34 needs to carry sulfated sialyl Lexis X (6-sulfo SLe<sup>X</sup>) epitopes on either core-1 or core-2 sugar structures.<sup>38</sup> As N-linked glycans seem to play no major role for the binding to L-selectin,<sup>39</sup> we focused our efforts here on the 70 potential extracellular O-linked glycosylation sites present in CD34. According to the predictions from the NetOGlyc server ([www.cbs.dtu.dk](http://www.cbs.dtu.dk)), the attachment of a sugar molecule to the oxygen of serine or threonine occurs at approximately 30 of these sites<sup>39</sup> and as many as fifteen are located in the fragment of human CD34 that is present in C7 but not in C6.

Combining three separate O-glycosylation prediction algorithms,<sup>40,41</sup> we mutated the three top hits (S109, T110, S123) in the R12 CAR C7 construct, either singly or in combination, to glutamine, giving rise to seven altered C7 hinges (S109Q, T110Q, S123Q, S109Q + T110Q, S109Q + S123Q, T110Q + S123Q, and S109Q + T110Q + S123Q). When expressed on primary T cells, R12 CAR constructs with altered

C7 hinges had transduction and MACS enrichment efficiencies comparable with those of their unaltered counterparts (data not shown). When co-cultured with ROR1<sup>+</sup> Mino cells, the R12 CARs with altered C7 hinges showed the same lytic capabilities as the original C7-hinged CARs, demonstrating that the S/T > Q substitutions did not render the CAR ineffective. However, when co-cultured with ROR1<sup>-</sup> MOLM-14 cells, the cells were still nonspecifically eliminated by ROR1 CARs with mutated C7 hinges, while the ROR1<sup>-</sup> Granta519 cells were not killed at all (Figure 4A).

To exclude that our prediction had missed a crucial O-glycosylation site, we mutated all 15 serine and threonine residues in C7, which were not present in C6, to glutamine. When introduced into the R12 CAR construct, the C7 15xQ hinge showed the same transduction efficiency, MACS enrichment efficacy and purity of the eluted fraction as the wild-type C7 hinge (data not shown). The lysis against ROR1<sup>+</sup> Mino cells was comparable to the lysis of C6- and C7-hinged R12 CARs, hence the cytotoxic capabilities were not altered by the 15 S/T > Q substitutions (Figure 4B). However, the unspecific lysis against ROR1<sup>-</sup> MOLM-14 cells still occurred, suggesting that the binding of the C7 hinge to its unknown target structure was not dependent on O-linked glycosylation of CD34. As the two MCL cell lines express L-selectin and also showed weak staining with an E-selectin mAb by flow cytometry and MOLM-14 cells analyzed in parallel stained negative (Figure 4C), we can exclude that selectins are the unknown structure(s) on MOLM-14 and other myeloid cells, which bind the C7 hinge in our CAR constructs.

#### Comparison of C6-hinged CD19 and CD33 CARs with their CD8-hinged counterparts

Some CAR constructs currently tested in clinical trials use a short hinge derived from the human CD8 $\alpha$  chain.<sup>2,42</sup> We therefore compared the killing efficacy and specificity of CD19 and CD33 CAR constructs with a C6 hinge to analogous constructs with a CD8 hinge. To enable selection of the CD8-hinged constructs with CD34 microbeads, primary human T cells were transduced with lentiviral vectors encoding BFP or  $\Delta$ CD34 in *cis* with C6- or CD8-hinged CD19 or CD33 CARs (Figure 5A), enriched via CD34 microbeads on MACS columns and then co-cultured with Mino, REH and MOLM-14 cells for 16 h. Mino cells, which express CD19 but not CD33 (Figure S1), were eliminated by C6- and CD8-hinged CD19 CARs, but not by CD33 CAR T cells (Figure 5B). Similarly, REH cells (CD19<sup>+</sup> CD33<sup>-</sup>, Figure S1) were efficaciously killed by both CD19 CAR T cells, however also experienced nonspecific toxicity of CD33-CD8h CAR T cells from two out of four healthy donors. A similar observation was not made with the corresponding C6-hinged CD33 CAR construct (Figure 5B). Finally, MOLM-14 cells, characterized by the absence of CD19 and high CD33 expression (Figure S1), were comparably lysed by both CD33 CARs but not by the CD19 CARs (Figure 5B).

When analyzing the culture supernatants, CD19 CAR T cells only secreted granzyme B, IFN- $\gamma$ , GM-CSF, TNF- $\alpha$  and IL-2 when cultured with the CD19<sup>+</sup> Mino and REH cells (Figure 5C).

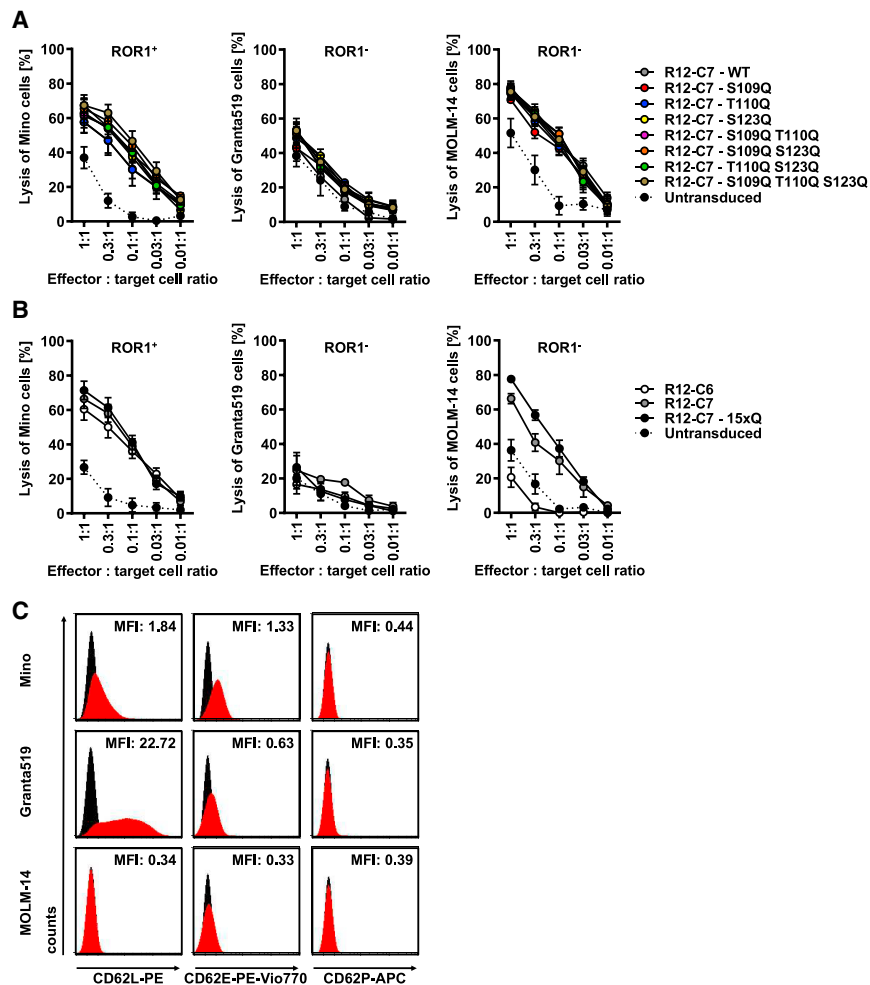


**Figure 4. Unspecific lysis by C7-hinged ROR1 CARs does not depend on O-glycosylation**

Primary human T cells were lentivirally transduced with VSVG-pseudotyped vectors encoding BFP in *cis* with C6-, C7- or mutated C7-hinged ROR1 CARs (clone R12). (A and B) Three days after transduction, the CAR T cells were enriched via MACS and subsequently co-cultured with EGFP-transduced Mino, Granta519 or MOLM-14 cells at decreasing effector-to-target cell ratios. After 16 h, the target cell lysis was assessed by flow cytometry. (C) Mino, Granta519 and MOLM-14 cells were stained with CD62L-PE, CD62E-PE-Vio770 and CD62P-APC and the antigen expression profiles were assessed by flow cytometry. P values were calculated by two-way ANOVA followed by Tukey's multiple comparison testing (A and B) and are summarized in Table S1. Data in (A) and (B) are presented as means  $\pm$  SEM of at least three biological replicates.

Interestingly, although Mino induced higher levels of granzyme B, IFN- $\gamma$  and GM-CSF, REH cells were more efficaciously killed. Although the CD33-CD8h CAR T cells eliminated REH cells at lower efficiencies (Figure 5B), this non-specific killing was not reflected in the cytokine secretion profiles (Figure 5C). In line with the cytotoxicity data, CD33 CAR T cells secreted, when co-cultured with MOLM-14 cells, granzyme B, IFN- $\gamma$ , GM-CSF and TNF- $\alpha$ . Interestingly only minimal amounts of IL-2 were detected here, when compared with the CD19 CAR T cells co-cultured with Mino or REH cells (Figure 5C). In summary, the C6 hinge proved to be as specific and efficacious as the CD8-derived hinge *in vitro*.

#### The C6 hinge can be used for a wide variety of CARs

Subsequently, we tested the usability of the C6 hinge for several CARs based on single scFVs against ROR1, CD5, CD19, CD33 and CD123. Primary human T cells were transduced with vectors encoding BFP in *cis* with C6-hinged CARs (Figure 5A), enriched via MACS, and co-cultured with Mino, JeKo-1, Granta519, MOLM-14, REH or Jurkat cells (see Figure S1 for the CD19,

CD5, ROR1, CD33 and CD123 cell-surface antigen expression profiles). When targeting ROR1, CAR T cells only eliminated cells of the ROR1<sup>+</sup> cell lines Mino and JeKo-1. CD5 CAR T cells efficaciously eliminated Mino and Jurkat cells and to a lesser extent JeKo-1 cells, which are only partially CD5<sup>+</sup>. CD19 CARs were effective in killing the CD19-expressing cell lines Mino, JeKo-1, Granta519 and REH, but not kill cells of the CD19<sup>-</sup> cell lines MOLM-14 and Jurkat. CD33 CAR T cells specifically eradicated MOLM-14 cells and CD123 CAR T cells eliminated Granta519 and MOLM-14 cells (Figure 6). Thus, all tested CARs were functional with our newly established C6 hinge and the killing characteristics of the various C6-hinged CAR T cells against

established hematopoietic cell lines strongly correlated with the antigen expression levels of the target antigens.

#### C6- and CD8-hinged CAR constructs mediate equal leukemia control *in vivo*

Finally, we explored the performance of the C6 hinge in xenotransplantation studies *in vivo*. Therefore, 8- to 10-week-old female NOD-SCID gamma (NSG) mice were xenografted with  $3 \times 10^6$  CD19<sup>+</sup> REH/ffluc-EGFP cells, expressing a fusion protein of human codon-optimized firefly luciferase and EGFP.<sup>43</sup> Seven days later,  $3 \times 10^6$  primary human T cells expressing BFP/CD19-C6,  $\Delta$ CD34/CD19-CD8h, BFP/CD33-C6 or  $\Delta$ CD34/CD33-CD8h constructs (Figure 5A) were intravenously injected after MACS enrichment without any conditioning (Figure 7A). Mice were monitored for the persistence and growth of REH/ffluc-EGFP cells at days 6, 14, 20, 28, and 38 via luminescence imaging and blood sample analysis (Figure 7). Mice in the control group (Untreated) showed the characteristic clinical presentation of a pre-B cell leukemia and had to be sacrificed between days 19 and 23 due to high disease burden (Figures 7A–7C).

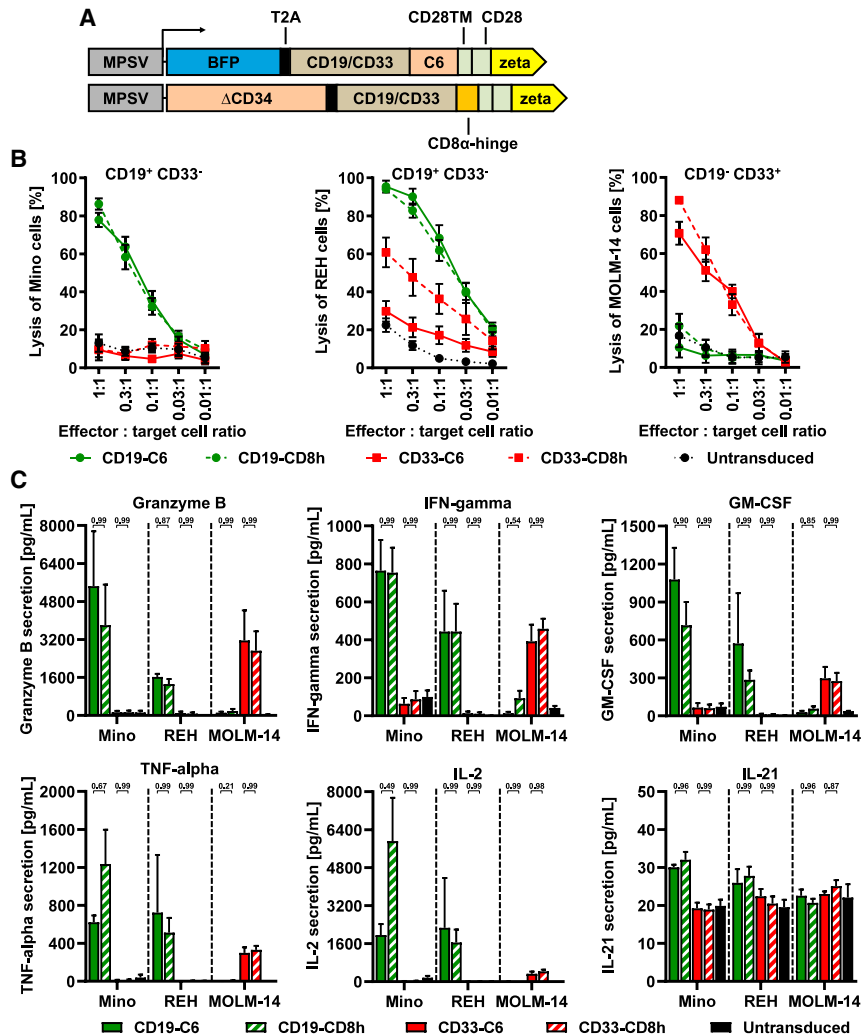


**Figure 5. C6-hinged CD19 and CD33 CAR constructs on T cells are as efficient as their CD8-hinged counterparts *in vitro***

Primary human T cells were lentivirally transduced with VSVG-pseudotyped vectors encoding BFP *in cis* with C6-hinged or ΔCD34 *in cis* with CD8-hinged CD19 or CD33 CARs (vectors depicted schematically in A). (B) Three days after transduction, the CAR T cells were enriched via MACS and subsequently co-cultured with EGFP-transduced Mino, REH and MOLM-14 cells at decreasing effector-to-target cell ratios. After 16 h, the target cell lysis was assessed by flow cytometry and (C) supernatants were harvested and analyzed for secretion of granzyme B, IFN- $\gamma$ , GM-CSF, IL-2, TNF- $\alpha$  and IL-21 via the MACSplex cytokine assay. p values were calculated by two-way ANOVA (B) or one-way ANOVA (C) followed by Tukey's or Dunnett's multiple comparison testing, respectively; asterisks indicate a p value of <0.05, and p values of lysis curves are summarized in Table S1. Data are presented as means  $\pm$  SEM of at least three biological replicates.

(Figure 7A). For both CD19 CAR constructs, it was possible to detect transduced T cells in the peripheral blood of animals by flow cytometry when staining with CD3-PerCP-Vio700, CD45-APC, and CD34-PE (QBend-10) antibodies. As a reflection of the *in vivo* expansion of the CD19 CAR T cells in reaction to the leukemia cell burden, mice initially even showed around 12% CD19-C6 and 10% CD19-CD8h CAR T cells in their peripheral blood, which decreased to around 2% and 0.5%, respectively, after 38 days (Figure 7E).

## DISCUSSION

Compared with other immunotherapies, autologous CAR T cells have shown an unprecedented efficacy for relapsed and/or refractory liquid malignancies of the B cell lineage.<sup>1</sup> This level of efficacy has been achieved with relatively simple overexpression strategies/vectors in simple treatment protocols and by targeting tumor-associated antigens (TAAs), for which the loss of the normal antigen-positive cells is clinically tolerated.<sup>1</sup> However, the future goals for CAR therapies must include to make these treatments more affordable and also effective for other malignancies, including solid tumors, where antigen heterogeneity and an immunosuppressive environment are major challenges.<sup>2</sup> In addition, using alternative allogeneic immune effector cells will require increased safety measures to prevent adverse immunological reactions, e.g., by inclusion of a suicide gene.<sup>44</sup> Thus, developing CAR therapies further will require more complex vector constructs with elements that have specific functions. With our CD34-derived 99 aa hinge C6, we have established an important hinge element for CARs that is functionally indistinguishable from the commonly used CD8 $\alpha$  hinge, but additionally facilitates antibody-based

Both CD33 CAR constructs (C6- or CD8-hinged) were not able to control the leukemia growth, and all animals in these two groups also had to be sacrificed between days 19 and 23, when the leukemia burden reached critical levels (Figures 7A–7C). For these three animal groups, we observed no CAR T cell persistence in the peripheral blood or bone marrow at sacrifice by flow cytometry, but detected a steadily increasing REH cell population in the blood (Figures 7D and 7E).

In contrast, mice that received CD19 CAR T cells showed a significantly prolonged survival and the persistence of REH/flluc-EGFP cells was markedly lower or even abolished, as shown via luminescence imaging and blood sample analysis (Figures 7A–7D). Importantly, the CD19-C6 CAR construct proved, with the exception of one animal in which we had problems during the CAR T cell injection, to be as efficient as the CD8-hinged counterpart construct by days 14 and 20. At days 28 and 38, we noted a recurrence/persistence of low levels of ALL cells in some NSG mice in CD19-C6 as well as CD19-CD8h animals

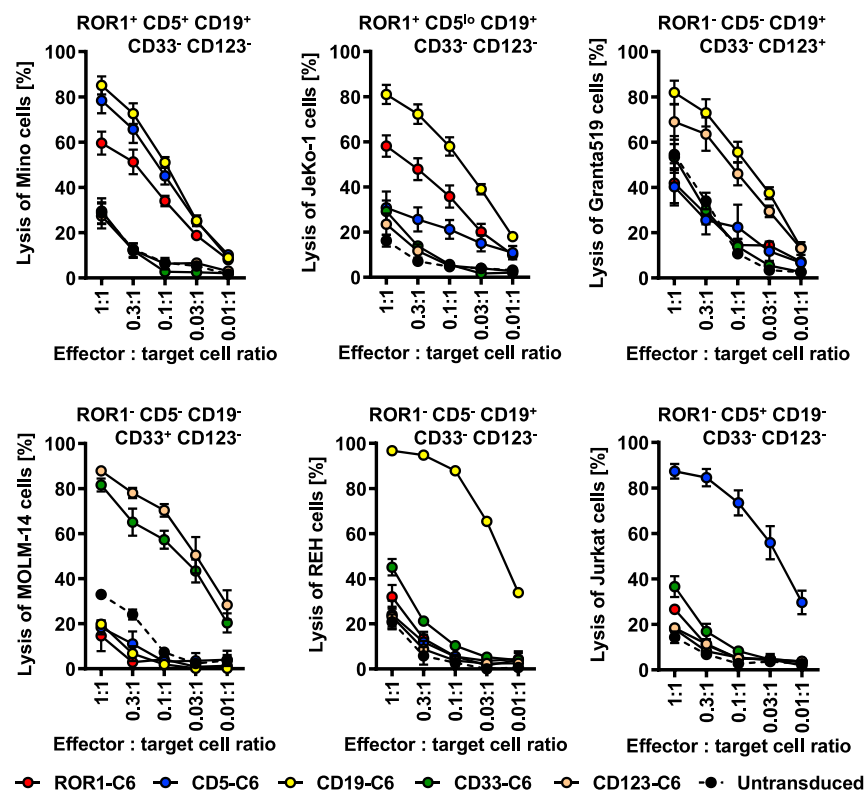


**Figure 6. The C6 hinge can be used for a variety of CARs against hematological malignancies**

Primary human T cells were lentivirally transduced with VSVG-pseudotyped vectors encoding BFP in *cis* with C6-hinged ROR1, CD5, CD19, CD33 or CD123 CARs. Three days after transduction, the CAR T cells were enriched via MACS and subsequently co-cultured with EGFP-expressing Mino, JeKo-1, Granta519, MOLM-14, REH or Jurkat cells at decreasing effector-to-target cell ratios. After 16 h, the target cell lysis was assessed by flow cytometry. *p* values were calculated by two-way ANOVA followed by Tukey's multiple comparison testing and are summarized in Table S1. Data are presented as means  $\pm$  SEM of at least three biological replicates.

CARs based on the mAbs 2A2 and R12 work best with a short hinge of 12 aa, as the epitopes of these two scFvs are located in the immunoglobulin-like domain located near the NH<sub>2</sub> terminus of ROR1, distal from the membrane.<sup>37</sup> In contrast, our R12 CAR T cells showed efficient lysis of ROR1<sup>+</sup> cells, irrespective of the incorporated hinge (99, 179 and 229 aa). One reason for these divergent results might be that, due to the MACS enrichment of genetically modified T cells providing us cells with high CAR expression levels, our CAR T cells are more efficient killers, especially considering that Hudecek et al. used effector-to-target cells ratios from 30:1 to 1:1, while ratios from 1:1 to 0.01:1 were sufficient in our cytotoxic assays. Two additional target antigen structures, where the hinge length appears to be critical for existing CARs using scFvs against membrane-proximal epitopes, are NCAM and the oncofetal antigen 5T4, both targetable with an IgG1-derived CH<sub>2</sub>CH<sub>3</sub> long hinge.<sup>8</sup> The glycosylation of the targeted antigen can be another factor where epitopes embedded within heavily glycosylated regions of a protein can only be targeted with long and flexible hinges. CARs against MUC1, whose glycosylation is frequently dysregulated in malignancies, also rely on the incorporation of a longer hinge derived from IgD (103 aa) to be functional.<sup>12</sup>

detection of CARs on transduced cells and microbead-mediated enrichment of genetically modified CAR effector cells to high purity under GMP conditions.

### Characteristics of the hinge

The majority of clinically tested and approved CAR products harbor hinges derived from CD8 or CD28,<sup>42</sup> which are, depending on which sequences are used, approximately 40–50 aa long.<sup>7,45</sup> Often, the epitopes in TAAs recognized by scFVs are located membrane-distal or are embedded within rather small antigen structures and therefore the CAR constructs do not need longer hinges. For example, the epitope for the high-affinity scFV of FMC63, the recognition unit for the most commonly studied CD19 CAR so far, is located in a membrane-distal area of CD19 and therefore readily accessible by CAR constructs with short as well as long hinges.<sup>8,11</sup> Still, certain scFVs exist where the length of the hinge is critical for efficient recognition of the TAA and killing of the target cells by CAR T cells. Hudecek et al.<sup>11</sup> demonstrated that ROR1 CARs derived from mAb clone R11, which binds an epitope of ROR1 in the Kringle domain close the cell membrane,<sup>37</sup> needs a full-length hinge (CH<sub>2</sub>CH<sub>3</sub>, 229 aa) to function properly. Reducing the hinge length to 119 or 12 aa completely abolishes the CAR-mediated cytotoxicity *in vitro* as well as *in vivo*.<sup>11</sup> These findings are in line with our data here, where the C6 (99 aa) and C7 (179 aa) hinges in the R11 CAR construct were insufficient to eliminate ROR1<sup>+</sup> MCL cells with R11 CAR T cells *in vitro*. In another study, Hudecek et al.<sup>10</sup> reported that ROR1

Casucci et al.<sup>19</sup> included surface sequences of the human low-affinity p75 NGFR into CAR constructs as hinge and demonstrated that NWL, the longest version (222 aa) with the complete extracellular sequence of NGFR, was best suited for both staining of transduced CAR T cells for flow-cytometric analysis and selection on MACS columns, albeit with a rather low yield of  $\leq 40\%$ . However, the authors did not compare the NGFR hinge with a standard hinge such as CD8, thus the feasibility of their hinge for clinical purposes is still unclear.

In contrast, we have shown here that our intermediate CD34 C6 hinge (99 aa) is an excellent candidate for a wide range of scFvs, as C6-hinged CAR constructs on CAR T cells show excellent efficacy against



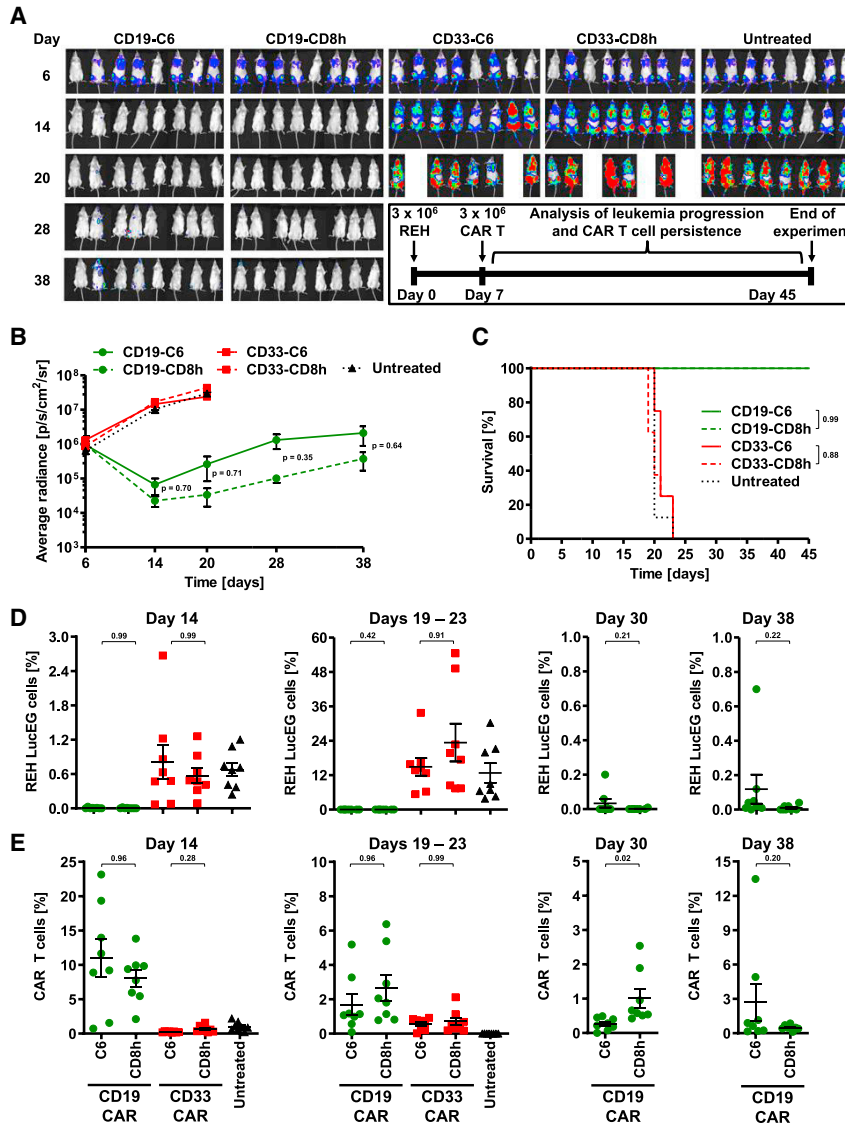


**Figure 7. C6-hinged CD19 CARs efficaciously control ALL disease progression *in vivo***

Primary human T cells were lentivirally transduced with VSVG-pseudotyped vectors encoding BFP in *cis* with C6-hinged or  $\Delta$ CD34 in *cis* with CD8-hinged CD19 or CD33 CARs. NSG mice (8 mice/group) were xenografted with  $3 \times 10^6$  cells of the human ALL cell line REH and received a single injection of  $3 \times 10^6$  MACS-enriched CAR T cells 7 days later. (A and B) At days 6, 14, 20, 28, and 38, mice were monitored for REH persistence via luminescence imaging. (C) Kaplan-Meier survival curves of the four treatment groups as well as the untreated mice. Blood samples were analyzed by flow cytometry on days 14, 19–23, 28 and 38 for (D) REH and (E) CAR T cell persistence. p values were calculated by mixed-model ANOVA followed by Tukey's multiple comparison testing (B), log-rank test (C), or one-way ANOVA followed by Dunnett's multiple comparison testing for days 14 and 19–23 or unpaired t test for days 30 and 38 (D and E). Data are presented as means  $\pm$  SEM.

QBend-10 and two epitopes for the rituximab mAbs in a single sequence placed on a CD8 $\alpha$ -derived stalk. Although the authors reported that transduced T cells can be enriched by using the CD34 MACS technology, the data presented on this topic in the paper is still sparse<sup>34</sup> and we can imagine, based on our own experiences in using the hinges C2–C4, that the CD34 microbeads-mediated selection of transduced T cells which harbor only short CD34 sequences is rather inefficient.

Here, we have established a novel hinge for CARs that allows rapid detection of CAR T cells, e.g. from peripheral blood and in functional analyses, and also efficient enrichment of the CAR T cells under GMP conditions prior to infusion into patients. Direct comparison of our C6 hinge and the widely used CD8 $\alpha$  hinge demonstrated *in vitro*, using numerous CARs and multiple leukemic cell lines, and *in vivo* in NSG mice that both hinges mediated similar cytotoxicities, that no non-specific off-target effects occur and that the cytokine profile of both hinges is identical. Interestingly, extending the C6 hinge by 80 additional amino acids (C7) was not possible, as we observed non-specific binding of C7-hinged CD19 and R12 CARs to AML-M4/M5 cell lines, similarly to what has been described for CARs containing CH<sub>2</sub>CH<sub>3</sub> hinges from human immunoglobulins.<sup>14</sup> Moreover, we recently demonstrated that our C6 hinge worked in CAR constructs recognizing solid tumor-associated antigens<sup>49,50</sup> and also here did not result in off-target activation of the genetically modified T cells, thus suggesting again that the C6 hinge seems to be well suited for CAR constructs for clinical products.

CD5, CD19, CD33, CD123 and ROR1 (R12) target antigens on malignant cells *in vitro* and also *in vivo* with CD19 CARs.

### Safety and clinical implications

The idea of including a marker that is not naturally expressed on the target cells in a CAR construct for selection of genetically modified cells for clinical settings is not new.<sup>46</sup> High purities and high yields are especially important if allogeneic donor T cells need to be controlled *in vivo* in patients, e.g. by co-expressing a suicide gene. Zhan et al.<sup>47,48</sup> used the surface and transmembrane sequences of human CD34 fused to the thymidine kinase enzyme of the herpes simplex virus for clinical safety testing of mismatched donor T cell infusions in patients after stem cell transplantation. Philip et al.<sup>34</sup> went one step further and created a highly compact sort/suicide gene by combining the binding epitope for the

In summary, we believe that our CD34-derived C6 hinge is an ideal candidate as an essential element for the next generations of CAR constructs, which need to contain additional functional elements to address the heterogeneity of antigen expression on the malignant cells and the tumor-associated immune suppression. These adoptive cellular therapies could also be combined with supportive or complementary treatment components in more complex protocols to influence the homeostasis in the tumor microenvironment and thus drive CAR T cell therapy forward.

## MATERIALS AND METHODS

### Construct generation

The self-inactivating (SIN) lentiviral vector for stable high-level co-expression of two transgenes in primary human T cells contains a *Thosea asigna* virus T2A site and the viral U3 regions from the myeloproliferative sarcoma virus (MPSV) as previously published.<sup>35</sup> The aa sequence for the different CD34-derived hinges C2–C7 were derived from a human codon usage-optimized version of truncated human CD34 (#P28906-2; GeneArt, Thermo Fisher Scientific, Schwerte, Germany).<sup>51</sup> The CD34-derived inserts were generated by PCR amplification and inserted into codon-usage optimized CD19 (clone FMC63) CAR vector.<sup>35</sup> For some constructs, we inserted the EGFP (#C5MKY7) as a fluorescent marker in front of the T2A site and different  $\Delta$ CD34-hinged CD19 CAR genes in second position after the T2A site. Moreover, the C6 and C7 hinges were inserted into codon-optimized CAR constructs against CD5 (clone H65<sup>52,53</sup>), ROR1 (clones R11 and R12<sup>10,11,37</sup>), CD33 (clone DRB2<sup>54</sup>) and CD123 (clone 43<sup>36</sup>) with the tagBFP marker being in 5' of the T2A site. When IgG4-derived CH<sub>2</sub>CH<sub>3</sub><sup>35</sup> or CD8-derived hinges were used in the CAR constructs, the truncated CD34 isoform ( $\Delta$ CD34) was inserted in front of T2A to enable CD34 microbead-mediated MACS enrichment of the genetically modified CAR T cells.

### Cell culture

All cell lines were obtained from DSMZ (Braunschweig, Germany) and grown in medium as recommended (DMEM GlutaMAX, RPMI1640 GlutaMAX, penicillin/streptomycin and fetal calf serum [FCS] were acquired from Thermo Fisher Scientific). Primary human T cells were collected from peripheral blood of healthy adult volunteers who gave informed consent according to the protocols (#4687 and #2019-623) approved by the local ethics committee (Universitätsklinikum Düsseldorf, Germany) and separated by density-gradient centrifugation using Ficoll-Paque (Cytiva Europe, Freiburg, Germany) according to the manufacturer's protocol. The PBMCs were cultivated on CD3- (Thermo Fisher Scientific) and CD28- (BD Biosciences, Heidelberg, Germany) coated nontissue culture-treated 6-well plates in Iscove's modified Dulbecco's medium (Sigma-Aldrich, Darmstadt, Germany) with 10% FCS, 100 U/mL penicillin, 100  $\mu$ g/mL streptomycin, 2 mM L-glutamine (all from Thermo Fisher Scientific) and 100 U/mL IL-2 (Proleukin, Novartis, Basel, Switzerland) to activate and specifically expand the T cells.

### Lentiviral vector production and transduction of eukaryotic cells

Vesicular stomatitis virus-G (VSV-G)-pseudotyped replication-deficient lentiviral particles were produced after transfection into HEK293T cells and used for transduction of cell lines and CD3/CD28-prestimulated primary human T cells in the presence of 10  $\mu$ g/mL protamine phosphate (Sigma-Aldrich) as described previously.<sup>55</sup>

### Cell enrichment

Three to four days after transduction, CAR T cells and Jurkat cells were enriched using CD34 microbeads based on the CD34 antibody QBend-10 (Miltenyi Biotec, Bergisch-Gladbach, Germany) according to the manufacturer's protocol. In brief, cells were stained with CD34 microbeads, loaded onto MS MACS columns, which were washed three times, and then eluted. The fractions (preMACS, flowthrough and postMACS) were analyzed by flow cytometry for EGFP, BFP and  $\Delta$ CD34 expression after staining with the QBend-10 CD34 antibody directly conjugated to phycoerythrin (PE) (Thermo Fisher Scientific). After enrichment on MACS columns, T cells were cultured for 1–2 days in 100 U/mL IL-2 until further usage or analysis.

### Functional *in vitro* cytotoxicity assays

Enriched and non-enriched CAR T cells were cultured with EGFP-expressing Mino, MOLM-14, REH, Granta519, JeKo-1, HL60, THP-1, LAMA84, MEG01, MONOMAC6, K562, and NB4 cells at various effector-to-target cell ratios in round-bottomed 96-well plates. After 16 h, the cultures were harvested, the cells incubated with propidium iodide for live/dead cell discrimination, and the samples analyzed on a MACSQuant-X (Miltenyi Biotec). EGFP expression was used to discriminate between effector and target cells. Samples with HL60, THP-1, LAMA84, MEG01, MONOMAC6, K562 and NB4 cells were stained with CD33-APC (Miltenyi Biotec) for discrimination between target and effector cells. The specific lysis was calculated as  $1 - (\text{number of viable GFP-positive cells}/\text{number of control GFP-positive cells}) \times 100\%$ . Negative lysis rates were set to 0%.

### Functional *in vitro* cytokine secretion assays

Cytokine secretion by CAR T cells was analyzed using the MACSPlex Cytotoxic T and NK Cell Kit (Miltenyi Biotec) according to the manufacturer's instructions. Supernatants for these analyses were collected after 16 h of co-cultivation of CAR T cells and the malignant target cells in round-bottomed 96-well plates at effector-to-target cell ratios of 1:1. The supernatants were stored at  $-20^{\circ}\text{C}$  until analysis. Per analysis, 50  $\mu$ L of undiluted supernatants was used.

### *In vivo* xenograft model

All *in vivo* studies were approved by the state animal research committee (LANUV, NRW, Germany) and animals were cared for according to guidelines of the Federation of European Laboratory Animal Science Associations. Eight- to ten-week-old female NSG mice (Charles River Laboratories, Sulzfeld, Germany) were xenografted with  $3 \times 10^6$  REH cells, stably expressing a human codon-optimized firefly luciferase-EGFP fusion protein (REH/ffluc-EGFP).<sup>43</sup> Seven days later,  $3 \times 10^6$  C6- or CD8-hinged CD19 or

CD33 CAR T cells were injected without conditioning. At days 6, 14, 20, 28 and 38, the persistence of REH cells was assessed by luminescence. Mice were injected with D-luciferin (OZ Biosciences, Marseilles, France) and the luciferase activity was measured after 5 min in a Caliper IVIS Lumina II system (PerkinElmer, Rodgau, Germany) with an exposure time of 15 s. Luminescence was analyzed using the Living Image software (PerkinElmer). At days 14, 19–23, 30 and 38, blood samples were analyzed by flow cytometry for persistence of REH and CAR T cells by assessing EGFP, CD19 and CD45 expression for REH cells and BFP, CAR ( $\Delta$ CD34), CD3 and CD45 expression for CAR T cells using CD34-PE, CD3-PerCP-Vio700, CD19-PE-Vio770 and CD45-APC directly conjugated monoclonal antibodies (the last three from Miltenyi Biotec), respectively.

### Statistical analysis

Statistical analysis was performed using GraphPad Prism 9.2.0. P values were, depending on experimental setup, calculated by unpaired t test, one-way analysis of variance (ANOVA), two-way ANOVA, mixed-model ANOVA, or log-rank test followed by Tukey's or Dunnett's multiple comparison testing where indicated. p values of lysis curves are summarized in Table S1, and p values less than 0.05 were considered statistically significant.

### SUPPLEMENTAL INFORMATION

Supplemental information can be found online at <https://doi.org/10.1016/j.omto.2021.11.003>.

### ACKNOWLEDGMENTS

We gratefully acknowledge the healthy donors who provided peripheral blood for the *in vitro* and *in vivo* studies. We would like to thank Jörg Schipper, MD, director of the ENT clinic, for his support of this research project. We are in debt to Wolfgang Schulz, PhD, and Michèle Hoffmann, PhD, both from the department of Urology, Heinrich Heine University, for the use of the MACSQuant-X. This work was supported, in part, by funding from the Medical Research School Düsseldorf, DSO, Heinrich-Heine-Universität Düsseldorf, Düsseldorf, the Essener Elterninitiative zur Unterstützung krebskranker Kinder e.V. and within the framework of the iCAN33 project, funded by the European Regional 470 Development Fund NRW (ERDF, German EFRE-0801320) 2014–2020.

### AUTHOR CONTRIBUTIONS

A.B., T.I., K.R., M.W., K.S., N.G., C.W., and H.H. planned the experiments. A.B., T.I., C.H., D.S., and K.R. conducted the experiments. A.B., T.I., C.H., K.R. and H.H. analyzed data. A.B., C.H., K.S., C.W., and H.H. wrote the manuscript. All authors approved the final manuscript.

### DECLARATION OF INTERESTS

H.H., C.W., T.I., and K.R. are inventors on a patent describing the CD34 hinge. All other authors declare no competing interests.

### REFERENCES

- June, C.H., and Sadelain, M. (2018). Chimeric antigen receptor therapy. *N. Engl. J. Med.* 379, 64–73. <https://doi.org/10.1056/NEJMr1706169>.
- Larson, R.C., and Maus, M.V. (2021). Recent advances and discoveries in the mechanisms and functions of CAR T cells. *Nat. Rev. Cancer* 21, 145–161. <https://doi.org/10.1038/s41568-020-00323-z>.
- Albinger, N., Hartmann, J., and Ullrich, E. (2021). Current status and perspective of CAR-T and CAR-NK cell therapy trials in Germany. *Gene Ther.* <https://doi.org/10.1038/s41434-021-00246-w>.
- Jonnalagadda, M., Mardiros, A., Urak, R., Wang, X., Hoffman, L.J., Bernanke, A., Chang, W.C., Bretzlaff, W., Starr, R., Priceman, S., et al. (2015). Chimeric antigen receptors with mutated IgG4 Fc spacer avoid fc receptor binding and improve T cell persistence and antitumor efficacy. *Mol. Ther.* 23, 757–768. <https://doi.org/10.1038/mt.2014.208>.
- Qin, L., Lai, Y., Zhao, R., Wei, X., Weng, J., Lai, P., Li, B., Lin, S., Wang, S., Wu, Q., et al. (2017). Incorporation of a hinge domain improves the expansion of chimeric antigen receptor T cells. *J. Hematol. Oncol.* 10, 68. <https://doi.org/10.1186/s13045-017-0437-8>.
- Watanabe, N., Bajgain, P., Sukumaran, S., Ansari, S., Heslop, H.E., Rooney, C.M., Brenner, M.K., Leen, A.M., and Vera, J.F. (2016). Fine-tuning the CAR spacer improves T-cell potency. *Oncoimmunology* 5, e1253656. <https://doi.org/10.1080/2162402X.2016.1253656>.
- Fujiwara, K., Tsunei, A., Kusabuka, H., Ogaki, E., Tachibana, M., and Okada, N. (2020). Hinge and transmembrane domains of chimeric antigen receptor regulate receptor expression and signaling threshold. *Cells* 9. <https://doi.org/10.3390/cells9051182>.
- Guest, R.D., Hawkins, R.E., Kirillova, N., Cheadle, E.J., Arnold, J., O'Neill, A., Irlam, J., Chester, K.A., Kemshead, J.T., Shaw, D.M., et al. (2005). The role of extracellular spacer regions in the optimal design of chimeric immune receptors: evaluation of four different scFvs and antigens. *J. Immunother.* 28, 203–211. <https://doi.org/10.1097/01.cji.0000161397.96582.59>.
- Moritz, D., and Groner, B. (1995). A spacer region between the single chain antibody- and the CD3 zeta-chain domain of chimeric T cell receptor components is required for efficient ligand binding and signaling activity. *Gene Ther.* 2, 539–546.
- Hudecek, M., Lupo-Stanghellini, M.T., Kosasih, P.L., Sommermeyer, D., Jensen, M.C., Rader, C., and Riddell, S.R. (2013). Receptor affinity and extracellular domain modifications affect tumor recognition by ROR1-specific chimeric antigen receptor T cells. *Cancer Res.* 19, 3153–3164. <https://doi.org/10.1158/1078-0432.CCR-13-0330>.
- Hudecek, M., Sommermeyer, D., Kosasih, P.L., Silva-Benedict, A., Liu, L., Rader, C., Jensen, M.C., and Riddell, S.R. (2015). The nonsignaling extracellular spacer domain of chimeric antigen receptors is decisive for *in vivo* antitumor activity. *Cancer Immunol. Res.* 3, 125–135. <https://doi.org/10.1158/2326-6066.CIR-14-0127>.
- Wilkie, S., Picco, G., Foster, J., Davies, D.M., Julien, S., Cooper, L., Arif, S., Mather, S.J., Taylor-Papadimitriou, J., Burchell, J.M., and Maher, J. (2008). Retargeting of human T cells to tumor-associated MUC1: The evolution of a chimeric antigen receptor. *J. Immunol.* 180, 4901–4909. <https://doi.org/10.4049/jimmunol.180.7.4901>.
- Almasbak, H., Walseng, E., Kristian, A., Myhre, M.R., Suso, E.M., Munthe, L.A., Andersen, J.T., Wang, M.Y., Kvalheim, G., Gaudernack, G., and Kyte, J.A. (2015). Inclusion of an IgG1-Fc spacer abrogates efficacy of CD19 CAR T cells in a xenograft mouse model. *Gene Ther.* 22, 391–403. <https://doi.org/10.1038/gt.2015.4>.
- Hombach, A., Hombach, A.A., and Abken, H. (2010). Adoptive immunotherapy with genetically engineered T cells: Modification of the IgG1 Fc 'spacer' domain in the extracellular moiety of chimeric antigen receptors avoids 'off-target' activation and unintended initiation of an innate immune response. *Gene Ther.* 17, 1206–1213. <https://doi.org/10.1038/gt.2010.91>.
- Turtle, C.J., Hanafi, L.A., Berger, C., Gooley, T.A., Cherian, S., Hudecek, M., Sommermeyer, D., Melville, K., Pender, B., Budiarto, T.M., et al. (2016). CD19 CAR-T cells of defined CD4+CD8+ composition in adult B cell ALL patients. *J. Clin. Invest.* 126, 2123–2138. <https://doi.org/10.1172/JCI85309>.
- Cerrano, M., Ruella, M., Perales, M.A., Vitale, C., Faraci, D.G., Giaccone, L., Coscia, M., Maloy, M., Sanchez-Escamilla, M., Elsbah, H., et al. (2020). The advent of CAR

- T-cell therapy for lymphoproliferative neoplasms: Integrating research into clinical practice. *Front. Immunol.* *11*, 888. <https://doi.org/10.3389/fimmu.2020.00888>.
17. Valton, J., Guyot, V., Boldajipour, B., Sommer, C., Pertel, T., Juillerat, A., Duclert, A., Sasu, B.J., Duchateau, P., and Poirot, L. (2018). A versatile safeguard for chimeric antigen receptor T-cell immunotherapies. *Sci. Rep.* *8*, 8972. <https://doi.org/10.1038/s41598-018-27264-w>.
  18. Koristka, S., Ziller-Walter, P., Bergmann, R., Arndt, C., Feldmann, A., Kegler, A., Cartellieri, M., Ehninger, A., Ehninger, G., Bornhauser, M., and Bachmann, M.P. (2019). Anti-CAR-engineered T cells for epitope-based elimination of autologous CAR T cells. *Cancer Immunol. Immunother.* *68*, 1401–1415. <https://doi.org/10.1007/s00262-019-02376-y>.
  19. Casucci, M., Falcone, L., Camisa, B., Norelli, M., Porcellini, S., Stornaiuolo, A., Ciceri, F., Traversari, C., Bordignon, C., Bonini, C., and Bondanza, A. (2018). Extracellular NGFR spacers allow efficient tracking and enrichment of fully functional CAR-T cells CO-expressing a suicide gene. *Front. Immunol.* *9*, 507. <https://doi.org/10.3389/fimmu.2018.00507>.
  20. Liu, L., Sommermeyer, D., Cabanov, A., Kosasih, P., Hill, T., and Riddell, S.R. (2016). Inclusion of Strep-tag II in design of antigen receptors for T-cell immunotherapy. *Nat. Biotechnol.* *34*, 430–434. <https://doi.org/10.1038/nbt.3461>.
  21. Maude, S.L., Frey, N., Shaw, P.A., Aplenc, R., Barrett, D.M., Bunin, N.J., Chew, A., Gonzalez, V.E., Zheng, Z., Lacey, S.F., et al. (2014). Chimeric antigen receptor T cells for sustained remissions in leukemia. *N. Engl. J. Med.* *371*, 1507–1517. <https://doi.org/10.1056/NEJMoa1407222>.
  22. Cruz, C.R., Micklethwaite, K.P., Savoldo, B., Ramos, C.A., Lam, S., Ku, S., Diouf, O., Liu, E., Barrett, A.J., Ito, S., et al. (2013). Infusion of donor-derived CD19-redirected virus-specific T cells for B-cell malignancies relapsed after allogeneic stem cell transplant: A phase I study. *Blood* *122*, 2965–2973. <https://doi.org/10.1182/blood-2013-06-506741>.
  23. Badbaran, A., Berger, C., Riecken, K., Kruchen, A., Geffken, M., Muller, I., Kroger, N., Ayuk, F.A., and Fehse, B. (2020). Accurate in-vivo quantification of CD19 CAR-T cells after treatment with axicabtagene ciloleucel (Axi-Cel) and tisagenlecleucel (Tisa-Cel) using digital PCR. *Cancers* *12*, 1970. <https://doi.org/10.3390/cancers12071970>.
  24. Zhang, Q., Hu, H., Chen, S.Y., Liu, C.J., Hu, F.F., Yu, J.M., Wu, Y.H., and Guo, A.Y. (2019). Transcriptome and regulatory network analyses of CD19-CAR-T immunotherapy for B-all. *Genomics Proteomics Bioinformatics* *17*, 190–200. <https://doi.org/10.1016/j.gpb.2018.12.008>.
  25. Keu, K.V., Witney, T.H., Yaghoubi, S., Rosenberg, J., Kurien, A., Magnusson, R., Williams, J., Habte, F., Wagner, J.R., Forman, S., et al. (2017). Reporter gene imaging of targeted T cell immunotherapy in recurrent glioma. *Sci. Transl. Med.* *9*, eaag2196. <https://doi.org/10.1126/scitranslmed.aag2196>.
  26. Jena, B., Maiti, S., Huls, H., Singh, H., Lee, D.A., Champlin, R.E., and Cooper, L.J. (2013). Chimeric antigen receptor (CAR)-specific monoclonal antibody to detect CD19-specific T cells in clinical trials. *PLoS One* *8*, e57838. <https://doi.org/10.1371/journal.pone.0057838>.
  27. Lee, D.W., Kochenderfer, J.N., Stetler-Stevenson, M., Cui, Y.Z.K., Delbrook, C., Feldman, S.A., Fry, T.J., Orentas, R., Sabatino, M., Shah, N.N., et al. (2015). T cells expressing CD19 chimeric antigen receptors for acute lymphoblastic leukaemia in children and young adults: A phase I dose-escalation trial. *Lancet* *385*, 517–528. [https://doi.org/10.1016/S0140-6736\(14\)61403-3](https://doi.org/10.1016/S0140-6736(14)61403-3).
  28. Chen, P.H., Lipschitz, M., Wright, K., Armand, P., Jacobson, C.A., Roberts, Z.J., Rossi, J.M., Bot, A., Go, W.Y., and Rodig, S.J. (2018). Analysis of CAR-T and immune cells within the tumor micro-environment of diffuse large B-cell lymphoma post CAR-T treatment by multiplex Immunofluorescence. *Blood* *132*. <https://doi.org/10.1182/blood-2018-99-113644>.
  29. Ayuk, F., Fehse, B., Janson, D., Berger, C., Riecken, K., and Kroger, N. (2020). Excellent proliferation and persistence of allogeneic donor-derived 41-BB based CAR-T cells despite immunosuppression with cyclosporine A. *Haematologica* *105*, E322–E324. <https://doi.org/10.3324/haematol.2019.245969>.
  30. Abramson, J.S., Palomba, M.L., Gordon, L.L., Lunning, M.A., Wang, M., Arnason, J., Mehta, A., Purev, E., Maloney, D.G., Andreadis, C., et al. (2020). Lisocabtagene marelucel for patients with relapsed or refractory large B-cell lymphomas (TRANSCEND NHL 001): A multicentre seamless design study. *Lancet* *396*, 839–852. [https://doi.org/10.1016/S0140-6736\(20\)31366-0](https://doi.org/10.1016/S0140-6736(20)31366-0).
  31. AbuSamra, D.B., Aleisa, F.A., Al-Amoodi, A.S., Jalal Ahmed, H.M., Chin, C.J., Abuelela, A.F., Bergam, P., Sougrat, R., and Merzaban, J.S. (2017). Not just a marker: CD34 on human hematopoietic stem/progenitor cells dominates vascular selectin binding along with CD44. *Blood Adv.* *1*, 2799–2816. <https://doi.org/10.1182/blood-advances.2017004317>.
  32. Shah, G.L., Scordo, M., Kosuri, S., Herrera, D.A., Cho, C., Devlin, S.M., Borrill, T., Carlow, D.C., AVECILLA, S.T., Meagher, R.C., et al. (2018). Impact of toxicity on survival for older adult patients after CD34(+) selected allogeneic hematopoietic stem cell transplantation. *Biol. Blood Marrow Transplant.* *24*, 142–149. <https://doi.org/10.1016/j.bbmt.2017.08.040>.
  33. Berger, M.D., Branger, G., Leibundgut, K., Baerlocher, G.M., Seipel, K., Mueller, B.U., Gregor, M., Ruefer, A., and Pabst, T. (2015). CD34<sup>+</sup> selected versus unselected autologous stem cell transplantation in patients with advanced-stage mantle cell and diffuse large B-cell lymphoma. *Leuk. Res.* *39*, 561–567. <https://doi.org/10.1016/j.leukres.2015.03.004>.
  34. Philip, B., Kokalaki, E., Mekkaoui, L., Thomas, S., Straathof, K., Flutter, B., Marin, V., Marafioti, T., Chakraverty, R., Linch, D., et al. (2014). A highly compact epitope-based marker/suicide gene for easier and safer T-cell therapy. *Blood* *124*, 1277–1287. <https://doi.org/10.1182/blood-2014-01-545020>.
  35. Roellecke, K., Virts, E.L., Einholz, R., Edson, K.Z., Altwater, B., Rossig, C., von Laer, D., Scheckenbach, K., Wagenmann, M., Reinhardt, D., et al. (2016). Optimized human CYP4B1 in combination with the alkylator prodrug 4-ypomeanol serves as a novel suicide gene system for adoptive T-cell therapies. *Gene Ther.* *23*, 615–626. <https://doi.org/10.1038/gt.2016.38>.
  36. Stein, C., Kellner, C., Kugler, M., Reiff, N., Mentz, K., Schwenkert, M., Stockmeyer, B., Mackensen, A., and Fey, G.H. (2010). Novel conjugates of single-chain Fv antibody fragments specific for stem cell antigen CD123 mediate potent death of acute myeloid leukaemia cells. *Br. J. Haematol.* *148*, 879–889. <https://doi.org/10.1111/j.1365-2141.2009.08033.x>.
  37. Yang, J., Baskar, S., Kwong, K.Y., Kennedy, M.G., Wiestner, A., and Rader, C. (2011). Therapeutic potential and challenges of targeting receptor tyrosine kinase ROR1 with monoclonal antibodies in B-cell malignancies. *PLoS One* *6*, e21018. <https://doi.org/10.1371/journal.pone.0021018>.
  38. Mitsuoka, C., Sawada-Kasugai, M., Ando-Furui, K., Izawa, M., Nakanishi, H., Nakamura, S., Ishida, H., Kiso, M., and Kannagi, R. (1998). Identification of a major carbohydrate capping group of the L-selectin ligand on high endothelial venules in human lymph nodes as 6-sulfo sialyl Lewis X. *J. Biol. Chem.* *273*, 11225–11233. <https://doi.org/10.1074/jbc.273.18.11225>.
  39. Hernandez Mir, G., Helin, J., Skarp, K.P., Cummings, R.D., Makitie, A., Renkonen, R., and Leppanen, A. (2009). Glycoforms of human endothelial CD34 that bind L-selectin carry sulfated sialyl Lewis x capped O- and N-glycans. *Blood* *114*, 733–741. <https://doi.org/10.1182/blood-2009-03-210237>.
  40. Steentoft, C., Vakhshushev, S.Y., Joshi, H.J., Kong, Y., Vester-Christensen, M.B., Schjoldager, K.T.B.G., Lavrsen, K., Dabelsteen, S., Pedersen, N.B., Marcos-Silva, L., et al. (2013). Precision mapping of the human O-GalNAc glycoproteome through SimpleCell technology. *Embo J.* *32*, 1478–1488. <https://doi.org/10.1038/emboj.2013.79>.
  41. Chauhan, J.S., Rao, A., and Raghava, G.P.S. (2013). In silico platform for prediction of N-, O- and C-glycosites in eukaryotic protein sequences. *PLoS One* *8*, e67008. <https://doi.org/10.1371/journal.pone.0067008>.
  42. Guedan, S., Calderon, H., Posey, A.D., Jr., and Maus, M.V. (2019). Engineering and design of chimeric antigen receptors. *Mol. Ther. Methods Clin. Dev.* *12*, 145–156. <https://doi.org/10.1016/j.omtm.2018.12.009>.
  43. Gu, D., Liu, H., Su, G.H., Zhang, X., Chin-Sinex, H., Hanenberg, H., Mendonca, M.S., Shannon, H.E., Chiorean, E.G., and Xie, J. (2013). Combining hedgehog signaling inhibition with focal irradiation on reduction of pancreatic cancer metastasis. *Mol. Cancer Ther.* *12*, 1038–1048. <https://doi.org/10.1158/1535-7163.MCT-12-1030>.
  44. Di Stasi, A., Tey, S.K., Dotti, G., Fujita, Y., Kennedy-Nasser, A., Martinez, C., Straathof, K., Liu, E., Duret, A.G., Grilley, B., et al. (2011). Inducible apoptosis as a safety switch for adoptive cell therapy. *N. Engl. J. Med.* *365*, 1673–1683. <https://doi.org/10.1056/NEJMoa1106152>.
  45. Alabanza, L., Pegues, M., Geldres, C., Shi, V., Wiltzius, J.J.W., Sievers, S.A., Yang, S.C., and Kochenderfer, J.N. (2017). Function of novel anti-CD19 chimeric antigen

- receptors with human variable regions is affected by hinge and transmembrane domains. *Mol. Ther.* 25, 2452–2465. <https://doi.org/10.1016/j.ymthe.2017.07.013>.
46. Bonini, C., Ferrari, G., Verzeletti, S., Servida, P., Zappone, E., Ruggieri, L., Ponzoni, M., Rossini, S., Mavilio, F., Traversari, C., and Bordignon, C. (1997). HSV-TK gene transfer into donor lymphocytes for control of allogeneic graft-versus-leukemia. *Science* 276, 1719–1724. <https://doi.org/10.1126/science.276.5319.1719>.
  47. Zhan, H., Gilmour, K., Chan, L., Farzaneh, F., McNicol, A.M., Xu, J.H., Adams, S., Fehse, B., Veys, P., Thrasher, A., et al. (2013). Production and first-in-man use of T cells engineered to express a HSVTK-CD34 sort-suicide gene. *PLoS One* 8, e77106. <https://doi.org/10.1371/journal.pone.0077106>.
  48. Eissenberg, L.G., Rettig, M.P., Ritchey, J.K., Prior, J.L., Schwarz, S.W., Frye, J., White, B.S., Fulton, R.S., Ghobadi, A., Cooper, M.L., et al. (2015). [(18)F]FHBG PET/CT imaging of CD34-TK75 transduced donor T cells in relapsed allogeneic stem cell transplant patients: Safety and feasibility. *Mol. Ther.* 23, 1110–1122. <https://doi.org/10.1038/mt.2015.48>.
  49. Haist, C., Schulte, E., Bartels, N., Bister, A., Poschinski, Z., Ibach, T.C., Geipel, K., Wiek, C., Wagenmann, M., Monzel, C., et al. (2021). CD44v6-targeted CAR T-cells specifically eliminate CD44 isoform 6 expressing head/neck squamous cell carcinoma cells. *Oral Oncol.* 116, 105259. <https://doi.org/10.1016/j.oraloncology.2021.105259>.
  50. Grunewald, C.M., Haist, C., König, C., Petzsch, P., Bister, A., Nößner, E., et al. (2021). Epigenetic priming of bladder cancer cells with decitabine increases cytotoxicity of human EGFR and CD44v6 CAR engineered T-cells. *Front. Immunol.* <https://doi.org/10.3389/fimmu.2021.782448>.
  51. Fehse, B., Richters, A., Putimtseva-Scharf, K., Klump, H., Li, Z., Ostertag, W., Zander, A.R., and Baum, C. (2000). CD34 splice variant: An attractive marker for selection of gene-modified cells. *Mol. Ther.* 1, 448–456. <https://doi.org/10.1006/mthe.2000.0068>.
  52. Mamonkin, M., Rouse, R.H., Tashiro, H., and Brenner, M.K. (2015). A T-cell-directed chimeric antigen receptor for the selective treatment of T-cell malignancies. *Blood* 126, 983–992. <https://doi.org/10.1182/blood-2015-02-629527>.
  53. Studnicka, G.M., Soares, S., Better, M., Williams, R.E., Nadell, R., and Horwitz, A.H. (1994). Human-engineered monoclonal antibodies retain full specific binding activity by preserving non-CDR complementarity-modulating residues. *Protein Eng.* 7, 805–814. <https://doi.org/10.1093/protein/7.6.805>.
  54. Stamova, S., Cartellieri, M., Feldmann, A., Arndt, C., Koristka, S., Bartsch, H., Bippes, C.C., Wehner, R., Schmitz, M., von Bonin, M., et al. (2011). Unexpected recombinations in single chain bispecific anti-CD3-anti-CD33 antibodies can be avoided by a novel linker module. *Mol. Immunol.* 49, 474–482. <https://doi.org/10.1016/j.molimm.2011.09.019>.
  55. Wiek, C., Schmidt, E.M., Roellecke, K., Freund, M., Nakano, M., Kelly, E.J., Kaisers, W., Yarov-Yarovoy, V., Kramm, C.M., Rettie, A.E., and Hanenberg, H. (2015). Identification of amino acid determinants in CYP4B1 for optimal catalytic processing of 4-ipomeanol. *Biochem. J.* 465, 103–114. <https://doi.org/10.1042/BJ20140813>.